Received: 8 September 2023 | Revised: 22 November 2023 | Accepted: 25 November 2023

DOI: 10.1002/pld3.555

RESEARCH ARTICLE

TurboID-mediated proximity labeling for screening interacting proteins of FIP37 in *Arabidopsis*

Xiaofang Li[1,2] | Yanping Wei[2] | Qili Fei[2] | Guilin Fu[2,3] | Yu Gan[2,4,5] | Chuanlin Shi[2]

[1]Shengzhou Research Base, State Key Laboratory of Cotton Biology, Zhengzhou University, Zhengzhou, China

[2]Shenzhen Branch, Guangdong Laboratory for Lingnan Modern Agriculture, Genome Analysis Laboratory of the Ministry of Agriculture, Agricultural Genomics Institute at Shenzhen, Chinese Academy of Agricultural Science, Shenzhen, China

[3]College of Agriculture, Shanxi Agricultural University, Taigu, China

[4]School of Life Sciences, Henan University, Kaifeng, China

[5]Shenzhen Research Institute of Henan university, Shenzhen, China

Correspondence
Chuanlin Shi, Shenzhen Branch, Guangdong Laboratory for Lingnan Modern Agriculture, Genome Analysis Laboratory of the Ministry of Agriculture, Agricultural Genomics Institute at Shenzhen, Chinese Academy of Agricultural Science, Shenzhen 518120, China.
Email: shichuanlin@caas.cn

Funding information
Chinese Postdoctoral Science Foundation, Grant/Award Number: 2021M703539; Training of Excellent Science and Technology Innovation talents in Shenzhen—Basic Research on Outstanding Youth, Grant/Award Number: RCYX 20200714114538196

Abstract

Proximity labeling was recently developed to detect protein–protein interactions and members of subcellular multiprotein structures in living cells. Proximity labeling is conducted by fusing an engineered enzyme with catalytic activity, such as biotin ligase, to a protein of interest (bait protein) to biotinylate adjacent proteins. The biotinylated protein can be purified by streptavidin beads, and identified by mass spectrometry (MS). TurboID is an engineered biotin ligase with high catalytic efficiency, which is used for proximity labeling. Although TurboID-based proximity labeling technology has been successfully established in mammals, its application in plant systems is limited. Here, we report the usage of TurboID for proximity labeling of FIP37, a core member of m^{6}A methyltransferase complex, to identify FIP37 interacting proteins in *Arabidopsis thaliana*. By analyzing the MS data, we found 214 proteins biotinylated by GFP-TurboID-FIP37 fusion, including five components of m^{6}A methyltransferase complex that have been previously confirmed. Therefore, the identified proteins may include potential proteins directly involved in the m^{6}A pathway or functionally related to m^{6}A-coupled mRNA processing due to spatial proximity. Moreover, we demonstrated the feasibility of proximity labeling technology in plant epitranscriptomics study, thereby expanding the application of this technology to more subjects of plant research.

KEYWORDS
biotin, m^{6}A, PL-MS, protein–protein interactions, TurboID

1 | INTRODUCTION

Proteins rarely function individually; more than 80% of proteins function by interacting with other molecules in cells (Berggard et al., 2007). Protein–protein interactions (PPIs) are an important basis for various life activities in cells, participating in a range of cellular processes, such as signal transduction, cell-to-cell communication, transcription, replication, and membrane transport (Keskin et al., 2016). Therefore, the interaction between intracellular proteins is of great significance for understanding the regulatory mechanisms of various biological processes. However, as the interactions between proteins are usually transient and weak, the study of PPIs is still a major challenge.

The traditional approaches of affinity purification and yeast two-hybrid (Y2H) have been widely applied to discover potential protein

interactions (Bruckner et al., 2009; Dunham et al., 2012). Antibody-based affinity purification, combined with mass spectrometry (MS)-based proteomics, ensures the endogenous proteins that interact with the bait proteins can be captured, identified, and quantified. However, this process has certain limitations. For example, the organelles or complexes studied must be extracted during cell or tissue lysis, followed by purification and washing steps. PPIs can be disrupted under the detergent conditions, and proteins located at different positions within the cell are mixed together during lysis; the interacting partners are extensively shuffled. This makes locating membrane-less organelles or protein complexes, such as membranes, chromatin, nuclear lamina, or cytoskeleton, more challenging (Gingras & Raught, 2012). Additionally, the nonspecific binding of proteins with antibodies or solid matrices tends to purify and identify proteins that do not specifically interact with the bait protein (Dunham et al., 2012). These background contaminants make it difficult to distinguish the true interactors from nonspecific interactions. Strict washing steps can be taken to minimize background interference; however, this tends to cause a loss of transient or weak interactions that might play important roles. Y2H is an in vivo genetic approach to discovering potential protein interactions based on the structure of transcription factors modules, and it is complementary compared with the emerging AP-MS technology. Y2H not only identifies direct interactions but also detects detect transient and low-affinity interactions (Gingras et al., 2019), but it cannot work for those organelle type proteins, which largely limits our understanding of cellular activity. In addition, the cDNA libraries used to construct Y2H are gene libraries, whereas some proteins are not suitable for Y2H detections, such as transcription factors (Fashena et al., 2000). Meanwhile, Y2H is difficult to study proteins associated with post-translational modifications, and the repeatability of Y2H results obtained in independent analysis is poor (Hamdi & Colas, 2012; Huang et al., 2007), and both the traditional AP-MS and Y2H assays are limited to the identification of PPIs in vitro or under nonphysiological conditions.

The recently developed proximity labeling technique overcomes the inherent limitations of traditional methods and is being gradually applied to the study of PPIs. Proximity labeling is generally conducted by fusing a catalytic enzyme to a protein of interest (bait protein) or anchoring it to a subcellular compartment (Yang et al., 2021). Because proximity labeling is performed in living cells in the native cellular environment, some false positives (artificial co-expression) and negatives (missing co-factors or scaffolds) can be avoided, and the weak and transient interacting proteins can be identified (Mair & Bergmann, 2022). At present, the enzymes commonly used in proximity labeling are the engineered soybean ascorbate peroxidase (APEX) (Martell et al., 2012) and a promiscuous mutant of *Escherichia coli* biotin ligase BirA (BioID) (Kim et al., 2016; Roux et al., 2012). APEX has high catalytic efficiency, but its effect requires the addition of a substrate molecule, hydrogen peroxide (H_2O_2), which is usually toxic to cells (Choi-Rhee et al., 2004). BioID is easier to introduce to the non-toxic biotin substrate, but its catalytic efficiency is too low, and the 18–24-h labeling time with biotin makes it difficult to study dynamic processes that occur transiently in cells. In addition, the optimal catalytic activity temperature of BioID is 37°C, which limits its application in plant systems, as most plants experience heat stress at this temperature (Zhang et al., 2019). TurboID and miniTurboID are biotin ligases designed by yeast-directed evolution from BirA with the R118G point mutation (Branon et al., 2018). TurboID can be fused with the target protein and expressed in cells. After that, the TurboID fusion protein catalyzes biotin to form reactive biotin-5′-AMP with the participation of ATP, which can promiscuously biotinylate the lysine residues of proteins, thus performing the biotin labeling of proximity proteins within about 10 nm (Roux et al., 2012). Then, biotin-tagged proteins are enriched and purified with streptavidin-conjugated magnetic beads, and identified by liquid chromatography–tandem MS (LC–MS/MS) (Branon et al., 2018; Gingras et al., 2019). So far, proximity labeling has been successfully applied to animal systems (Batsios et al., 2016; Branon et al., 2018; Opitz et al., 2017) and plant systems (Arora et al., 2020; Mair et al., 2019; Mair & Bergmann, 2022; Zhang et al., 2019), demonstrating the utility and versatility of proximity labeling in life science. However, the application of proteomic approaches in plants presents unique challenges compared with animals, including a low cytoplasmic volume relative to cell wall mass, high protease and phosphatase content, and ribulose-1,5-bisphosphate carboxylase/oxygenase (RuBisCo), which may interfere with protein detection and identification (Khan et al., 2018; Liu et al., 2015). Thus, the application of TurboID-based proximity labeling in plant systems has yet to be optimized.

More than 170 post-transcriptional modifications have been identified in RNAs, including N^6-methyladenosine (m^6A), N^1-methyladenosine (m^1A), 5-methylcytosine (m^5C), 5-hydroxymethylcytosine (hm^5C) and pseudouridine (ψ) (Frye et al., 2018; Yue et al., 2019). The m^6A methylation modifications are widely present in tRNA, mRNA, miRNA, long-coding RNA and snRNA (Boccaletto et al., 2018) and have important biological functions, including RNA splicing (Alarcon et al., 2015), mRNA nuclear export (Fustin et al., 2013), selective polyadenylation (Ke et al., 2015), translation (Zhao et al., 2017), and miRNA biogenesis (Bhat et al., 2020). This modification widely regulates RNA post-transcriptional fate, plant growth development, stress responses, and other life activities (Hu et al., 2021; Shen et al., 2016).

FIP37 (FKBP12 interacting protein, WTAP human homologous protein) is a core component of the *Arabidopsis* m^6A methyltransferase complex. Knockout of *FIP37* in *Arabidopsis* results in delayed endosperm development and subsequent embryonic lethality, with markedly reduced m^6A modifications levels (Vespa et al., 2004; Zhong et al., 2008). Further studies found that the m^6A pathway also interact with proteins in the light-regulated circadian clocks pathway in plants. For example, blue light-activated CRY2 protein forms photobodies through phase separation to recruit m^6A methyltransferase complex, and interacts with MTA, MTB, and FIP37 to regulate the abundance of mRNA methylation and the circadian rhythm in plants (Wang et al., 2021). This shows that FIP37 plays an important role in m^6A methylation. In addition, ZC3H13 is a critical regulatory protein in m^6A methylation and affects mESC (mouse embryonic stem cell) pluripotency through interacting with WTAP, Virilizer, and HAKAI and regulating their localization in animals (Knuckles et al., 2018; Wen et al., 2018).

However, there is no homologous protein of ZC3H13 in plants, suggesting that plants may have unique components yet to be found.

In this study, we wonder if fusing the TurboID to FIP37 could capture transient and dynamic interacting proteins of FIP37 in *Arabidopsis*. By using TurboID-based proximity labeling with MS (PL–MS), we identified numbers of interacting protein candidates with FIP37, including the known components of the m^6A methyltransferases complex, such as MTA, MTB, VIR, HAKAI, and HIZ1. These findings confirm that TurboID is a powerful proximity labeling approach with high sensitivity. Thus, our study demonstrates that TurboID-based proximity labeling is a simple and rapid technique for efficient screening of proximal and interacting proteins in plants.

2 | MATERIALS AND METHODS

2.1 | Plasmid construction

The TurboID fragment (TurboID from V5-TurboID-NES_pCDNA3) was amplified by polymerase chain reaction (PCR) and then digested with XbaI and SpeI, respectively. It was then ligated into the SpeI/XbaI-digested *35S::GFP-3xFLAG* (reconstructed form pCAMBIA1300 vector) vector to generate the plasmid *35S::GFP-TurboID-3xFLAG*. Using *Arabidopsis* cDNA as a template, the gene *FIP37* was amplified by PCR. The resulting fragment was transformed by homologous recombination into the *35S::GFP-TurboID-3xFLAG* vector, which had been digested with SpeI and AscI, to generate the plasmid *35S::GFP-TurboID-FIP37-3xFLAG*. DNA sequencing was performed to confirm all the plasmids. All primers are listed in Table S3.

2.2 | *Nicotiana benthamiana* infiltration

The above vector was transformed into *Agrobacterium* (GV3101). The *Agrobacterium* were inoculated in 20 ml of LB medium and incubated at 28°C for 16 h. Cultured cells were harvested and resuspended (10-mM MES [pH 5.6], 10-mM $MgCl_2$, and 150-μM acetosyringone) to an OD_{600} of 1. pSoup-p19 (tomato bushy stunt virus [TBSV] protein p19) was mixed in a 1:1 proportion and infiltration into four-week-old *Nicotiana benthamiana* leaves (grown in a greenhouse with 16-h light and 8-h photoperiod at 28°C). Expression was confirmed using a fluorescence microscope after 36–48 h, and leaves were harvested with a puncher, merging five disks per sample. The samples were then rapidly immersed in 50-μM biotin solution, quickly vacuum infiltrated until the leaves were filled with liquid, with water submerged leaves as a control. After treatment, the leaves were rapidly frozen in liquid nitrogen and stored at −80°C.

2.3 | Protein extraction and biotin activity assay

Plant tissue was ground with liquid nitrogen and 500-μl protein extraction buffer (50-mM Tris–HCl [pH 7.5], 150-mM NaCl, 5-mM $MgCl_2$, 10% glycerol, .1% NP-40, .5-mM DTT, 1-mM PMSF, 1× protease inhibitor cocktail) was added to each sample. The protein mixture was placed on ice for 30 min and reversed several times every 5 min, then centrifuged at 13,000*g* for 20 min. The supernatants were mixed with 5× sodium dodecylsulphate (SDS) loading buffer and heated at 98°C for 10 min. Protein expression was detected by anti-GFP antibody (TransGen Biotech, Catalog number HC201-02), and biotinylated protein were detected by streptavidin-HRP (Thermo Fisher Scientific, Catalog number S911).

2.4 | Generation of transgenic *Arabidopsis* lines

Transformation of *Arabidopsis thaliana* was performed via the floral dip method using *Agrobacterium tumefaciens* strain GV3101 (Harrison et al., 2006). Briefly, *Arabidopsis* plants were grown for approximately 4 weeks until they reached the vigorous flowering period. Meanwhile, *35S::GFP-TurboID-FIP37-3xFLAG* and *35S::GFP-TurboID-3xFLAG* vectors were transformed into *Agrobacterium*, inoculated in 20 ml of LB medium at 28°C for 16 h, centrifuged at 5000*g* for 10 min, and resuspended in 5% sucrose with $OD_{600} = 1$. Silwet was added prior to infection, and *Arabidopsis* flowers were immersed in the broth for 1 min, dark cultured for 1 day after infection, and harvested after seeds matured.

Seeds were surface sterilized by immersion in 75% (v/v) ethanol for 2 min, followed by immersion in 10% (v/v) sodium hypochlorite solution for 10 min, and washed five to six times with sterile distilled water. The seeds were then subjected to low temperature treatment for 2–3 days at 4°C. The seeds were sown in 1/2 Murashige and Skoog plates containing antibiotics (carbenicillin: 100 μg/ml, hygromycin: 50 μg/ml), and placed in a growth chamber for 4–6 h at 22°C under continuous light.

The plates were wrapped in aluminum foil and incubated for 48 h at 22°C. The aluminum foil was removed and seedlings were incubated for 24–48 h at 22°C under continuous light. Transgenic seedlings could be identified by hypocotyl elongation and the growth of green leaves. The positive seedlings were then transplanted to soil and screened for homozygous *Arabidopsis* lines in the next generation.

2.5 | TurboID sample preparation for MS analysis

Arabidopsis seeds were sown on 1/2 Murashige and Skoog plates containing .5% sucrose under long day conditions (16 h light/8 h dark, 22°C) for 5 days. The 5-day-old *Arabidopsis* transgenic seedlings of GFP-TurboID and GFP-TurboID-FIP37 overexpression were treated with 50 μM of biotin and vacuum infiltrated under the plant tissue, which was filled with liquid (this process took approximately 10 min). The seedlings were then incubated at room temperature (~22°C) for 3 h, with GFP-TurboID overexpression lines used as negative controls. There were two biological replicates, each weighing approximately .8-g fresh weight. After treatment, the plant material was quickly washed three times in ice-cold water to stop the labeling reaction and

to remove excess biotin, then dried and flash-frozen. Samples were quickly ground to powder in liquid nitrogen and resuspended in 4 ml of protein extraction buffer (50-mM Tris–HCl [pH 7.5], 150-mM NaCl, .5% sodium deoxycholate, .1% SDS, 1-mM EDTA, 1% Triton X-100, 1 mM DDT, 1-mM PMSF, leupeptin, protease inhibitor cocktail). The resuspension was centrifuged at 17,000*g* for 15 min at 4°C to remove cell debris. The supernatant was transferred to a fresh tube and centrifuged again for 15 min, and a small amount of the supernatant was taken as an input.

The desalting column (Thermo Fisher Scientific, Catalog number 89893) was equilibrated with 5-ml protein extraction buffer three times, and the protein extracts were then placed in the column to remove excess free biotin. To enrich biotinylated proteins from protein extracts, the desalted proteins were added to the 120-µl Dynabead C1 streptavidin beads (Invitrogen, Catalog number 65001) and incubated on a rotator wheel overnight (12–16 h) at 4°C. The next day, the beads were separated from the protein extracts on a magnetic rack and subsequently washed twice with 1-ml protein extraction buffer, once with 1 M KCl buffer, once with 100 mM Na_2CO_3 buffer, and once with buffer (1 M Urea add to 10 mM Tris–HCl) and finally twice with 1-ml protein extraction buffer. To confirm the successful enrichment of the biotinylated proteins, 20 µl of beads were taken out with 4x SDS loading buffer (200 mM Tris–HCl [pH 6.8], 8% SDS, 40% Glycerol, 20% β-mercaptoethanol, .1% Bromophenol blue, 2 mM Biotin, 20 mM DDT) and heated at 95°C for 5 min for Western Blot analysis. The rest of the beads were flash-frozen in liquid nitrogen and stored at −80°C or immediately sent on dry ice for LC–MS/MS analysis.

2.6 | Biotinylated proteins digestion

The streptavidin beads that were enriched with biotinylated proteins were eluted by 4× SDS loading buffer and heated at 95°C for 5 min, then the eluted proteins were separated by SDS-PAGE gels. The protein gel was stained with decoloring solution and reduced with reduction solution 1 (10-mM DTT and 25-mM NH_4HCO_3) at 55°C for 1 h, and then alkylated with reduction solution 2 (50-mM iodoacetamide and 25-mM NH_4HCO_3) in the dark for 30 min. Finally, .02-µg/µl trypsin was added and the digest completed by an overnight (16 h) incubation at 37°C. The digested peptides were extracted with peptide extraction buffer (5% formic acid and 67% acetonitrile) for 20 min at 37°C and dried in a vacuum concentrator. The dried peptides samples were resuspended in .1% formic acid, followed by desalting on Ziptip C18 resins twice. The desalted peptides were dried in a speed vacuum and used for subsequent MS analysis.

2.7 | MS analysis

For MS analysis, the dried peptides samples were resuspended in nano-high-performance liquid chromatography (HPLC) Buffer A (.1% formic acid) and separated using the Nano-HPLC liquid phase system EASY-nLC1200. Trap column (100 µm × 20 mm, RP-C18, Thermo Scientific) were balanced at 100% liquid A (.1% formic acid). The sample was adsorbed onto Trap column and then separated by the Analysis column (75 µm × 150 mm, RP-C18, Thermo Scientific). The flow rate was 300 nl/min and a 30-min gradient was used. The enzyme products were separated by capillary HPLC and then analyzed by mass spectroscopy using a Q-Exactive mass spectrometer (Thermo Scientific). The mass spectrometer was operated in data-dependent acquisition mode, and the top 20 most intense precursor ions were chosen for high-energy collision dissociation (HCD) fragmentation following a full scan. The peptides were fragmented with HCD and normalized collision energy (NCE)28. MS1 spectra were measured at a resolution of 70,000, an automatic gain control (AGC) of 3e6 with a maximum ion time of 100 ms. MS2 spectra were measured at a resolution of 17,500, an AGC of 1e5 with a maximum ion time of 50 ms.

The MS raw data for each sample were searched using the Proteome Discover 2.5 software against a Uniprot-*Arabidopsis thaliana* database. Precursor and fragment mass error tolerances were set at 10 ppm (ppm) and .05 Da, respectively. Trypsin was chosen as the enzyme with a maximum of two missed cleavages. Carbamidomethyl (C) was set as a static modification while acetyl (Protein N-term), deamidated (NQ), and oxidation (M) were set as a dynamic modification. All matched MS spectra were filtered by mass accuracy and matching scores to reduce protein false discovery rate (FDR) (strict) to ≤.01 or .01 < FDR (relaxed) < .05 on the basis of the target-decoy strategy using a reversed database.

2.8 | Gene ontology/KEGG enrich analysis

The software R was used to assess the enrichment of differential proteins, with defined adjusted *p* value of <.5. Enrichment analysis and drawing were performed by the clusterProfiler and ggplot packages, respectively. In the KEGG enrichment map, each cycle represents an enriched pathway, and the size of the cycles is proportional to the total number of genes in each pathway.

2.9 | Luciferase (Luc) complementation image assay

FIP37 and 10 candidate interacting proteins were fused with the C-terminal and N-terminal of firefly luciferase, respectively, and the fusion vector was transferred into *Agrobacterium* GV3101. The *Agrobacterium* was then co-infiltrated into tobacco leaves using an injection syringe. After approximately 48 h, luciferin was sprayed on the leaves and the fluorescence was quenched for several minutes in the dark. The luciferase signal was visualized using a Chemiluminescence Imaging System.

2.10 | Yeast two-hybrid assays

The full-length coding sequence of FIP37 was cloned by PCR. We constructed the vector pGBKT7-FIP37 and pGADT7-cDNA libraries that were co-transformed into the yeast strains, followed by toxicity

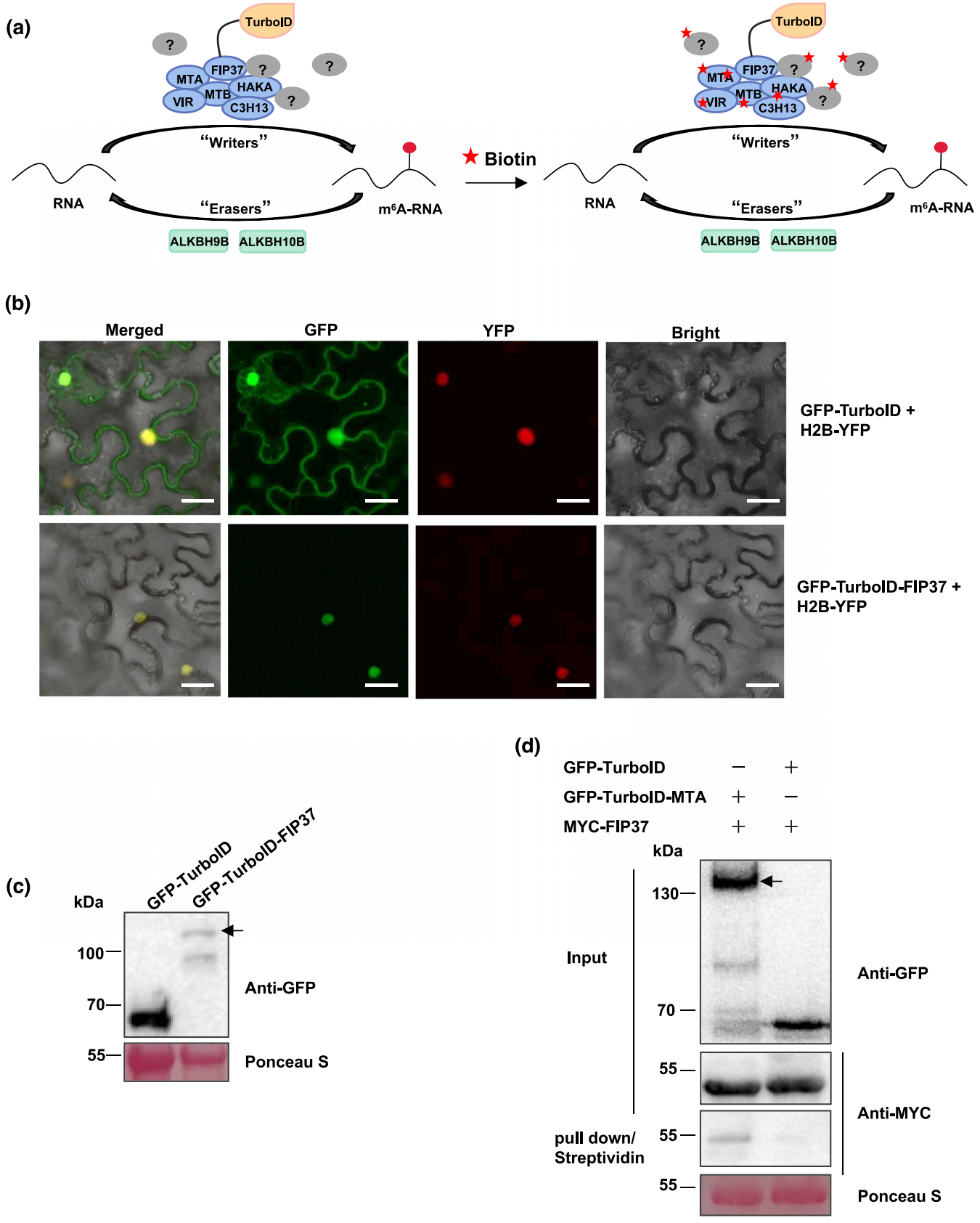

FIGURE 1 Legend on next page.

FIGURE 1 Validation of the efficacy of TurboID-mediated proximal labeling. (a) The schematic diagram of screening system for FIP37 based on TurboID-mediated proximity labeling. (b) Subcellular co-localization of H2B-YFP with GFP-TurboID and GFP-TurboID-FIP37 in *Nicotiana benthamiana* leaves. Scale bar, 25 μm. (c) Immunoblot analysis for protein expression in (b). The molecular weight size markers in kDa are indicted at the left. The arrow indicates the FIP37-fusion band. (d) Streptavidin pull-down analysis of the interaction between MTA and FIP37 by using TurboID. GFP-TurboID-MTA or GFP-TurboID was co-infiltrated with MYC-FIP37 into *N. benthamiana* leaves. Western blot analysis of the total input proteins with anti-GFP, anti-MYC. Western blot analysis of the streptavidin pull-down with anti-MYC. The arrow indicates the MTA-fusion band. Ponceau S staining served as loading control of the input.

assays and self-activation assays. Positive yeast clones were selected in SD/-trp/-leu/-his medium, and then cultured in SD/-trp/-leu/-his/-ade/A/X-α-Gal medium. Subsequently, growing positive clones were selected for PCR and Sanger sequence alignment using NCBI to annotate the candidate targets.

3 | RESULTS

3.1 | TurboID vector construction and proximity labeling efficacy validation

To construct a TurboID-based proximity labeling tool with which to screen interacting proteins of FIP37 (Figure 1a), we first added GFP and FLAG tags to the N- and C-terminus of TurboID, respectively, to generated the *35S::GFP-TurboID-3xFLAG* fusion as the negative control (referred to as GFP-TurboID hereafter). Then, we cloned the full-coding sequence of *FIP37* and inserted it into GFP-TurboID to generated the *35S::GFP-TurboID-FIP37-3xFLAG* fusion (referred to as GFP-TurboID-FIP37 hereafter) (Figure 1a and Figure S1). Next, we detected their expression with H2B (nuclear marker) (International Rice Genome Sequencing, 2005) through transient expression in *N. benthamiana* leaves using *Agrobacterium*-mediated infiltration. Subcellular localization showed that GFP-TurboID was localized in both the cytoplasm and the nucleus, while GFP-TurboID-FIP37 was predominantly localized in the nuclear (Figure 1b). The theoretical sizes of GFP-TurboID and GFP-TurboID-FIP37 are 70.2 and 108.2 kDa, respectively. An immunoblotting assay with an anti-GFP antibody showed that they were expressed in expected sizes (Figure 1c).

After that, we investigated whether the TurboID has biotin ligase activity on FIP37 using TurboID-fused MTA. MTA is a known member of m^6A methyltransferase that interacts with FIP37 in *Arabidopsis* (Zhong et al., 2008). We cloned the full-length coding sequence of *MTA* to generated the construct *35S::GFP-TurboID-MTA-3xFLAG* fusion (referred to as GFP-TurboID-MTA hereafter) and constructed MYC-tagged fusion (referred to as MYC-FIP37 hereafter) (Figure S2). These two constructs were co-expressed in *N. benthamiana* leaves. In addition, GFP-TurboID was also co-expressed with GFP-TurboID-MTA as the negative control. After 36 h of infection, agroinfiltrated leaves were infiltrated with 200-μM biotin for 3–12 h prior to harvesting. To determine whether FIP37 was biotinylated, the total protein extracts of tobacco leaves were pulled down by streptavidin beads. Immunoblot assays showed that all the fusion proteins were successfully expressed in the input, and FIP37 can be pulled down by streptavidin beads (Figure 1d). These results confirm that GFP-TurboID-MTA can efficiently ligate biotin to FIP37, suggesting that TurboID-based proximity labeling can be applied to detect the interacting proteins of m^6A methyltransferase in plant cells.

3.2 | Effect of biotin labeling concentration and time

To identify FIP37 interacting proteins through proximity labeling, we developed transgenic *Arabidopsis* overexpressing GFP-TurboID-FIP37 and GFP-TurboID. Confocal microscopy confirmed that the localization of GFP-TurboID-FIP37 fusion protein was localized in the nucleus in *Arabidopsis* root, while GFP-TurboID was localized in both the cytoplasm and the nucleus (Figure 2a), consistent with the results in tobacco. Western blot analysis with an anti-GFP antibody further confirmed that both constructs were successfully expressed in *Arabidopsis* (Figure 2b).

It was previously reported that there is no difference in the catalytic efficiency of TurboID between 22°C and 30°C (Mair et al., 2019), and room temperature can be used for TurboID-mediated labeling in *Arabidopsis*. Other than the temperature condition, the optimal time and concentration of biotin treatment is also the key factors to influence the efficiency of TurboID-based proximity labeling in plant cells. Therefore, we tested a concentration gradient of biotin in 5-day-old seedlings of GFP-TurboID and GFP-TurboID-FIP37 to determine the optimal exogenous biotin concentration. Seedlings were immersed in biotin solution with a concentration gradient from 10 to 250 μM by brief vacuum treatment for 10 min. To detect the biotinylated proteins, we extracted the total protein of seedlings. Western blot analysis showed that the most labeling bands were visible with 10-μM biotin treatment. These became saturated with 50-μM biotin; thereafter, no new bands emerged with a higher concentration in both GFP-TurboID and GFP-TurboID-FIP37 (Figure 2c). These results indicated that the optimal concentration of biotin treatment is 50 μM and that the efficiency of labeling was not increased with a higher concentration of biotin.

We also tested the optimal incubation time on TurboID-mediated protein biotinylation because having too short labeling time might not be sufficient to biotinylate proximal proteins, whereas having too long labeling might tend to increase biotinylation, giving rise to excessive false-positive signals. Thus, we established different biotin incubation times to determine the optimal incubation time by using 5-day-old seedlings of GFP-TurboID and GFP-TurboID-FIP37. Our results showed that protein biotinylation

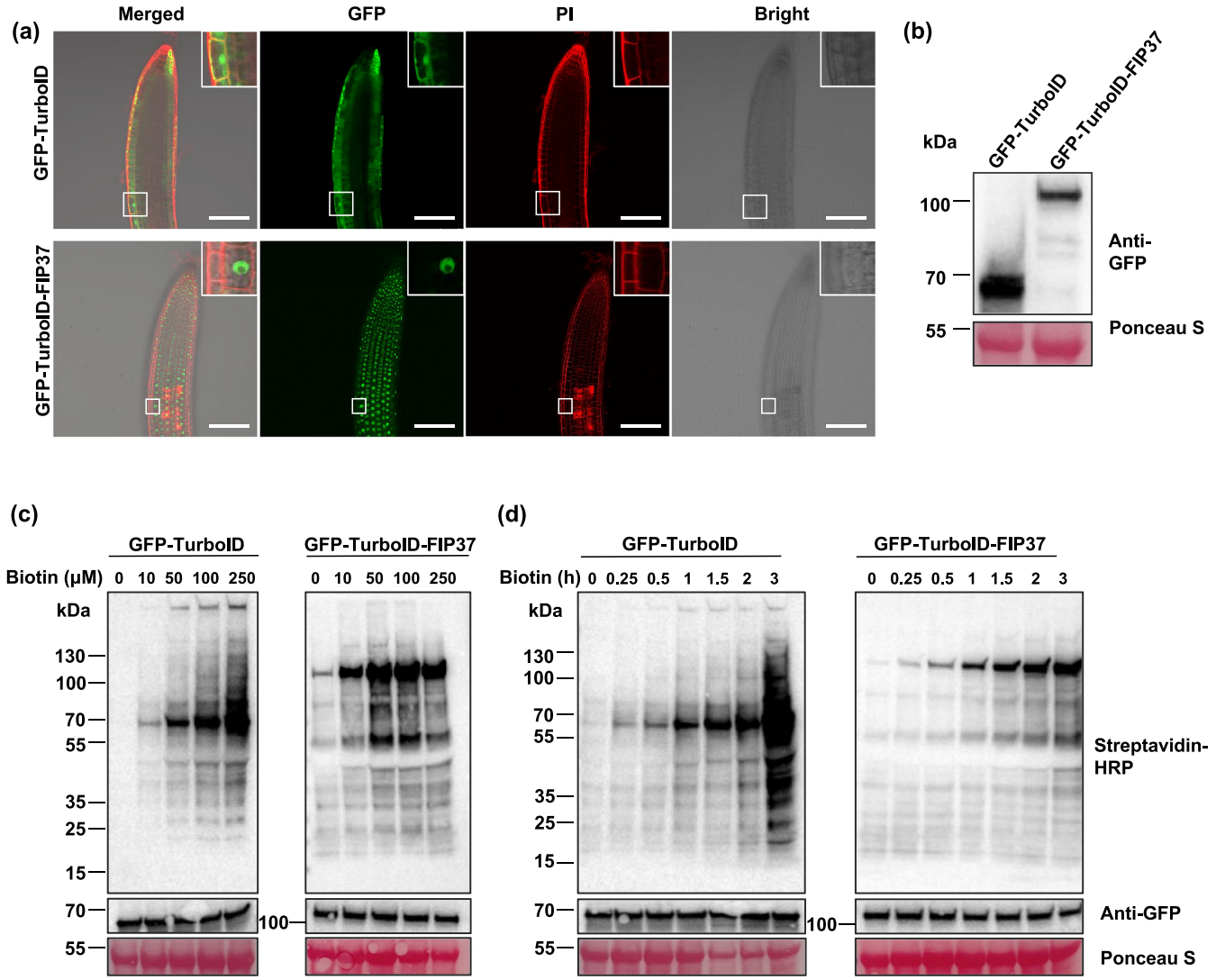

FIGURE 2 The effect of promiscuous biotin concentration and incubation time on TurboID-based proximity labeling in *Arabidopsis* seedlings. (a) Subcellular location of GFP-TurboID and GFP-TurboID-FIP37 in *Arabidopsis*. Roots of 7-day-old seedlings grown on 1/2 MS medium were observed confocally. Scale bar, 50 μm. PI, propidiumlodidie. (b) Immunoblot analysis of protein expression shown in part (a). (c) Identification of the optimal biotin concentration for TurboID-based biotinylation in 5-day-old seedlings of GFP-TurboID and GFP-TurboID-FIP37 transgenic *Arabidopsis*. (d) The effect of incubation time of promiscuous biotin applied to GFP-TurboID and GFP-TurboID-FIP37. Ponceaus staining shows the loading of the input.

reached saturation for 60 min, and 3 h incubation time could increase the amount of detected protein without a new protein band emerging (Figure 2d).

3.3 | Identification of FIP37 interacting protein using PL–MS

Next, we sought to identify the FIP37 interacting protein using the TurboID-based proximity labeling tool for FIP37, followed by LC–MS/MS. Although biotinylated protein can be detected after a short period of biotin treatment, 50-μM biotin treatment for 3 h is more appropriate for LC–MS/MS analysis according to the previous study (Mair et al., 2019). Therefore, we treated the GFP-TurboID and GFP-TurboID-FIP37 overexpression *Arabidopsis* seedlings with 50-μM biotin for 3 h, and samples of two biological replicates were collected for each transgenic line. Total protein was extracted from plant tissues, and free biotin was removed by desalting columns. Then, extracting proteins were incubated with streptavidin C1 beads. The beads were washed, then protein was eluted and analyzed by LC–MS/MS. MS identified 558 and 658 proteins from these two replicates of GFP-TurboID-FIP37 samples (Figure 3a), including the known m^6A methyltransferase MTA, MTB, VIR, HAKAI, and HIZ1 (Hu et al., 2021; Zhang et al., 2022; Zhong et al., 2008), which further confirms that our experimental proximity labeling can successfully identify true interacting proteins of the bait protein. Therefore, it is reasonable to speculate that the PL–MS-identified proteins potentially contain novel proteins that interact with FIP37. We

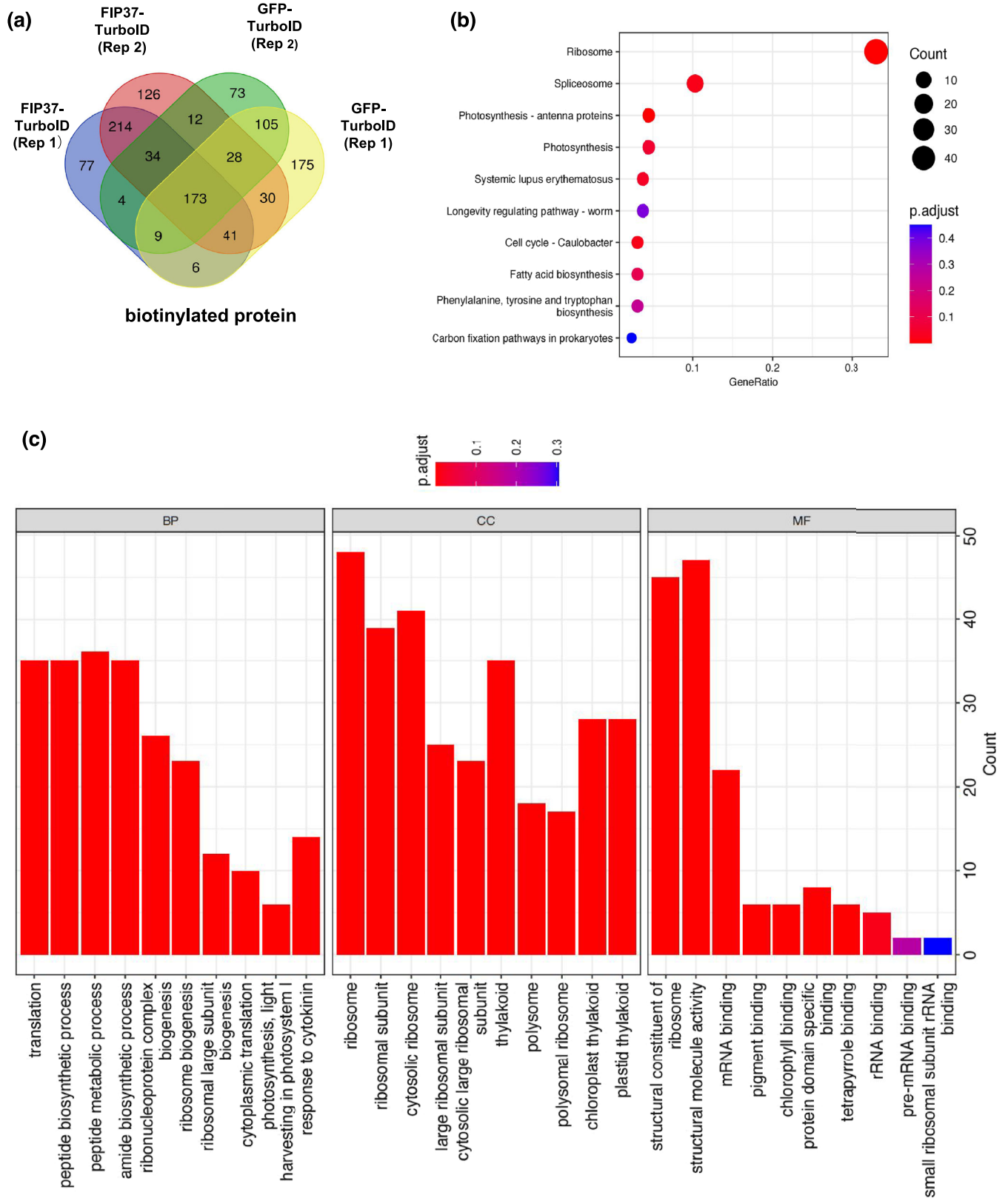

FIGURE 3 Identification of FIP37 interacting proteins using proximity labeling with mass spectrometry (PL–MS). (a) Venn diagrams showing the overlap of proteins that interact with FIP37. GFP-TurboID-FIP37 (left) and GFP-TurboID (right) have two independent biological replicates. (b) KEGG enrichment analysis for specific FIP37 interacting proteins compared with control. The size of the circle represents the number in each term. (c) GO enrichment analysis for specific FIP37 interacting proteins compared with control. CC, BP, and MF refer to cellular component, molecular function, and biological process, respectively.

propose that the protein list might serve as a useful resource to explore the multifaceted functions of the m^{6}A methyltransferase machinery in plants.

By comparing the identified proteins with the GFP-TurboID, we were able to eliminate nonspecific biotinylated proteins and obtain a more confident list with 214 proteins that potentially interact with FIP37 (Figure 3a, Table S1). To predict the relevant biological functions, cellular localization, and molecular processes of these proteins, we performed Kyoto Encyclopedia of Genes and Genomes (KEGG) enrichment analysis and Gene Ontology (GO) analysis. We found that these proteins are involved in a variety of cellular functions, such as splicing and RNA processing, which is related to the known function of FIP37 in mRNA regulation (Figure 3b,c). Moreover, ribosome-related proteins account for a large proportion (53 out of 214), possibly because the synthesis of the ribosome subunit is located in the nucleolus, consistent with the subcellular localization of FIP37. These results suggest that FIP37 might also play a role in rRNA biogenesis and metabolism, potentially regulating downstream protein translation.

3.4 | Verification of proximal proteins of FIP37

Next, we validated whether the FIP37 interacting proteins identified from TurboID-based proximity labeling are bona fide interactors of FIP37. Considering the nuclear localization of FIP37, we distinguish 214 proteins according to their subcellular localization, including nucleus, cytosol, chloroplast, mitochondrion, plasma membrane, ribosome. Out of the 214 proteins, 72 are predicted to be nucleus localized as shown in the Table S1. These nucleus-localized proteins are more likely to interact with FIP37. Then, considering the function of FIP37 as m^{6}A methyltransferase, the selected proteins should be involved in RNA transcription, RNA processing, DNA replication, RNA stability, translation, and RNA structure. Finally, in order to prove the credibility of the results, selected proteins should have high confidences with FDR ≤ .01 in the PL–MS analysis. Therefore, we selected seven proteins for subsequent verification. We performed firefly luciferase (Luc) complementation analysis to detect the interactions between these candidate proteins with FIP37 in vivo. FIP37 was fused to C-terminal Luc (CLuc), while the candidates were fused to N-terminal Luc (NLuc). The CLuc and NLuc constructs were transiently co-expressed in *N. benthamiana* leaves, and the luciferase signal was observed 48 h after inoculation.

We served luciferase signals in six proteins, namely, ALYS (AT1G66260), T31P16.50 (AT5G10060), PAPS19 (AT1G17980), SRZ22 (AT4G31580), ATZR-1C (AT5G04280), and SAP18 (AT2G45640), suggesting that these proteins can interact with FIP37 in vivo (Figure 4). In contrast, the luciferase signal for IRP9 (AT4G25550) was negative, confirming that this protein may not directly interact with FIP37. Taken together, these results demonstrated that the proximity labeling approach is highly efficient for the screening of m^{6}A methyltransferase PPIs in plants.

3.5 | Comparison of Y2H and PL–MS

In addition to proximity labeling with PL–MS, yeast two-hybrid (Y2H) is a traditionally powerful tool for the identification of PPIs. Therefore, we also attempted to screen for FIP37 interacting proteins using Y2H. A total of 34 positive clones were identified by FIP37-Y2H screening (Figure S5), and were subsequently characterized by Sanger sequencing. Of these, 27 proteins were functionally annotated by sequence comparison against the NCBI database, with four categorized as unknown proteins. Considering the subcellular localization and function of FIP37, eight of them were predicted to exhibit nuclear localization and more likely to interact with FIP37. Next, we selected three proteins to perform firefly luciferase complementation analysis. Our results showed that DUF2361 (AT1G04230), RH35 (AT5G5128), and NTF2 (AT5G60980) could all be observed luciferase signals (Figure 5a), suggesting that these three proteins could interact with FIP37 in vivo.

Our results showed that only three proteins were identified in both Y2H and proximity labeling (Figure 5b), namey, LHCA3 (AT1G61520), PSBO1 (AT5G66570), and TUA5 (AT5G19780). Fewer overlapping proteins were detected, which might be due to the limitations of Y2H in detecting the transient, indirect and weak interactions as FIP37 plays a complex and dynamic role in living cells. In terms of the number of interacting proteins detected for FIP37, proximity labeling seems to be more advantageous. Therefore, TurboID-based proximity labeling is an important supplement to traditional technology in the study of PPIs.

4 | DISCUSSIONS

PPIs are essential to various life activities in cells. The analysis of PPIs using high-throughput screening is important in understanding the regulatory mechanisms of various biological processes. In the past, affinity purification methods such as co-Immunoprecipitation (co-IP) and traditional biochemical research methods relying on yeast hybrid systems have been widely used. However, these methods are not effective in discovering transient and weak interactions in vivo. Proximity labeling, on the other hand, does not require the destruction of cells for complex separation and has become a powerful tool for detecting PPIs in various species. Thus, it overcomes the limitations of traditional technologies (Chen et al., 2015; Roux et al., 2012).

Because protein structures and their interactions are very dynamic and may change even within a certain time window, proximity labeling can detect more transient and weak interactions in the cell, while Y2H is more suitable for detecting strong and stable protein interactions. If the protein interactions are extremely weak or transient, then Y2H may not be able to detect their interactions. We identified 214 and 17 FIP37 interacting proteins by proximity labeling with PL–MS and Y2H, respectively, and only three overlapping proteins were identified in both methods. Considering that FIP37 acts as one key member of m^{6}A methyltransferase to involve in RNA

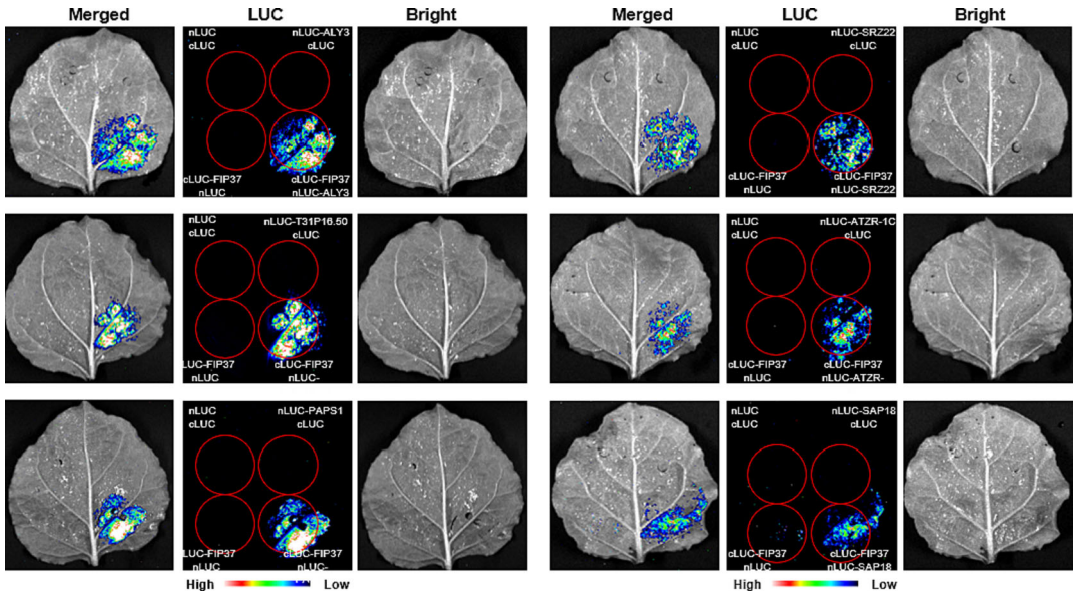

FIGURE 4 Confirmation of FIP37 interacting proteins by Luc in vivo. Luc complementation imaging assays between FIP37 and ALY3, T31P16.30, PAPS1, SRZ22, ATZR-1C, and SAP18, respectively.

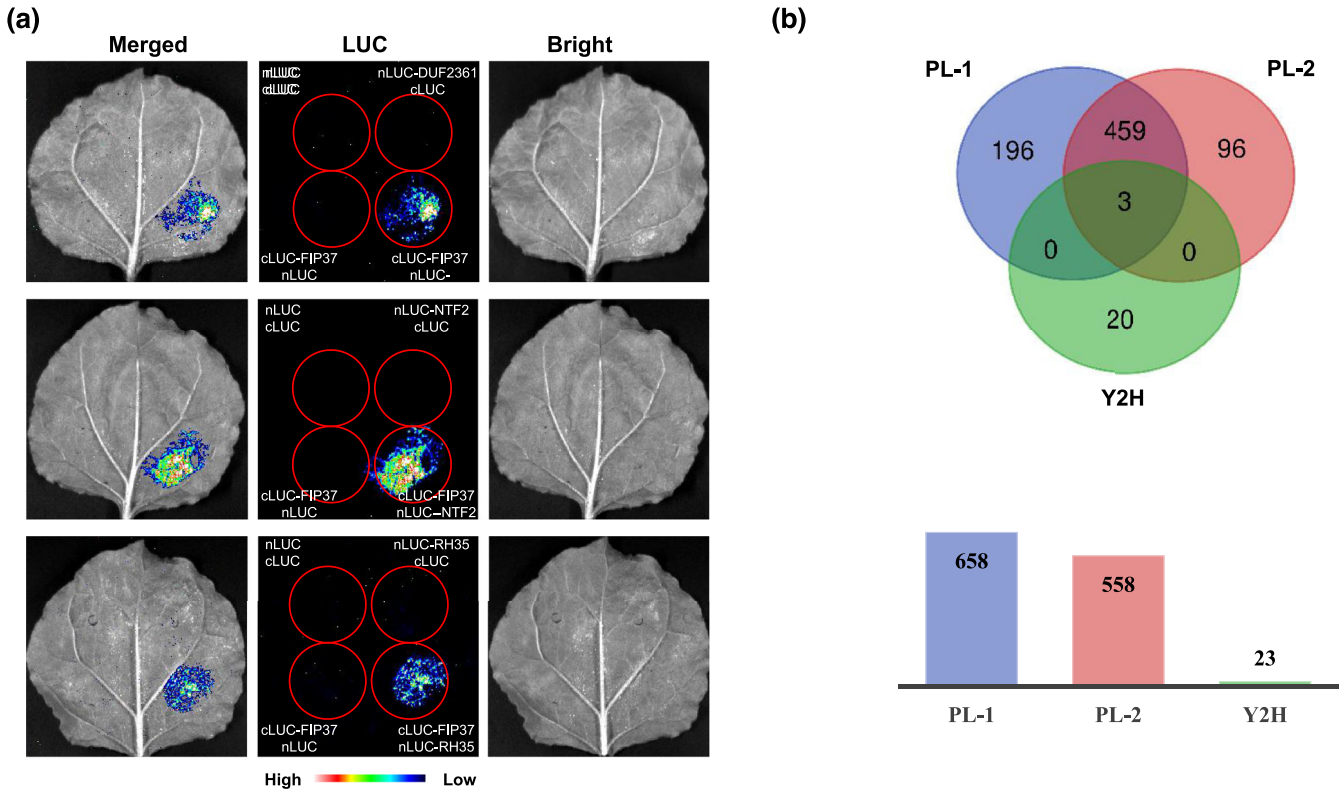

FIGURE 5 Two methods for screening FIP37 interacting proteins. (a) Confirmation of protein interactions between FIP37 and DUF2361, NTF2, RH35 by Luc complementation imaging assays in vivo. (b) Venn diagram showing overlap between PPI identification for FIP37 by proximity labeling (PL) and Y2H.

processing. In RNA stability and translation, its functions are complex and dynamic in living cells, which might lead to fewer proteins are detected by Y2H. In terms of the number of interacting proteins detected for FIP37, proximity labeling identified proteins about 20 times larger than Y2H, suggesting proximity labeling being more advantageous. Therefore, proximity labeling is an ideal method for identifying the low-affinity, transient PPIs or insoluble protein structures in the native cellular environment. However, this application has

not been used extensively in plants. Therefore, we used the m^{6}A methyltransferase FIP37 to demonstrate the application of TurboID-mediated proximity labeling in *Arabidopsis*.

We observed a small degree of labeling before providing exogenous biotin, suggesting that TurboID can utilize low levels of biotin in the growing cell or organism, but this is not sufficient for optimal biotin labeling and requires the addition of exogenous biotin. Besides, some biotinylated proteins could be detected even in the wild type without biotin incubation (Mair et al., 2019). Comparing the number and size of the biotin-labeled proteins after biotin treatment, we observed a significant increase in the number of biotinylated protein bands expressing GFP-TurboID-FIP37, indicating that the TurboID fusion proteins in plants have catalytic activity and allow biotinylated labeling of neighboring proteins. In addition, the number of captured proteins is closely related to the conditions of the proximity labeling assay. High activity and rapid labeling can lead to nonspecific labeling, so we tested the optimal biotin labeling time and concentration. Although TurboID can be labeled within 15 min, biotin itself is non-toxic, and it is available within 3 h of biotin labeling for proteins that require longer observation periods. Second, biotinylation is induced by the addition of exogenous biotin, which produces abundant free biotin during labeling. Plant tissues also carry free biotin into extracts that compete for binding to streptavidin C1 beads. To effectively enrich biotin, the protein must be desalted to remove free biotin and then incubated with the magnetic beads. This can be achieved by using a desalting column, which greatly improves the efficiency of the pulldown. Our experiments show that the protein is unaffected after desalination (Figure S4).

We established an appropriated negative control GFP-TurboID to eliminate false positives. The extremely high affinity between streptavidin and biotin can result in amplification of Western blot signals due to multiple binding sites with streptavidin for highly biotinylated proteins. Additionally, proximity labeling requires the fusion of biotin ligase with bait proteins, which may affect function, localization, and even interaction, and the constructed fusions need to be transiently or stably transfected into cells for overexpression, which may result in over labeling and false-positive results. Furthermore, although biotin ligase has the ability to capture weak and transient protein interactions, the identified interactions are not limited to directly bound proteins, so a negative control is necessary.

Studies have shown that proximity labeling is a powerful tool that can be used to analyze the proteomes of specific cell types in plants, map subcellular protein and transcription, and identify protein membrane topology and surface-exposed protein subunits (Yang et al., 2021). It also helps to research the subcellular spatial location and interaction of not only for proteins but also for RNA and DNA (Ramanathan et al., 2018; Schmidtmann et al., 2016). However, proximity labeling also has some disadvantages, as it requires the produce of transgenic plants, limiting the range of plants to which it can be applied such as rice and corn.

According to our study, some new FIP37 interacting proteins, such as ALYS, T31P16.50, PAPS19, SRZ22, ATZR-1C, SAP18, DUF2361, RH35, NTF2, and LHCA3, may mediate m^{6}A pathway-related functions. These proteins are worth being studied in future research. The application of proximity labeling also is worth popularizing in species other than model plants, such as rice, wheat, and maize. In general, we demonstrated the effectiveness of TurboID-based PL–MS as a tool with which to study the subcellular proteome of plants, complementing traditional methods of identifying PPIs. TurboID-based proximity labeling provides an additional tool for reliably and conveniently identifying the interacting partners of target proteins in plants. The discovery and optimization of various enzymes have driven the rapid development of proximity labeling, which has the potential to greatly improve our understanding of plant proteomics and is likely to play an increasingly important role.

AUTHOR CONTRIBUTIONS

Chuanlin Shi and Qili Fei designed the experiments and provided supervision. Xiaofang Li, Yanping Wei, and Guilin Fu conducted all the experiments. Xiaofang Li, Yanping Wei, and Yu Gan helped with data analysis. Xiaofang Li, Qili Fei and Chuanlin Shi wrote the manuscript. All authors have read and agreed to the published version of the manuscript.

ACKNOWLEDGMENTS

This research was funded by the Chinese Postdoctoral Science Foundation (2021M703539), the Training of Excellent Science and Technology Innovation talents in Shenzhen—Basic Research on Outstanding Youth (RCYX 20200714114538196). The author are grateful for the research platform from Agricultural Genomics Institute at Shenzhen, Chinese Academy of Agricultural Sciences.

CONFLICT OF INTEREST STATEMENT

Authors declares no conflict of interest.

DATA AVAILABILITY STATEMENT

The MS data have been submitted to ProteomeXchange via PRIDE Archive with the dataset identifier PXD043041.

PEER REVIEW

The peer review history for this article is available in the Supporting Information of this article.

ORCID

Chuanlin Shi https://orcid.org/0000-0003-4776-1942

REFERENCES

Alarcon, C. R., Goodarzi, H., Lee, H., Liu, X., Tavazoie, S., & Tavazoie, S. F. (2015). HNRNPA2B1 is a mediator of m(6)A-dependent nuclear RNA processing events. *Cell*, *162*(6), 1299–1308. https://doi.org/10.1016/j.cell.2015.08.011

Arora, D., Abel, N. B., Liu, C., Van Damme, P., Yperman, K., Eeckhout, D., Vu, L. D., Wang, J., Tornkvist, A., Impens, F., Korbei, B., Van Leene, J., Goossens, A., De Jaeger, G., Ott, T., Moschou, P. N., & Van Damme, D. (2020). Establishment of proximity-dependent biotinylation approaches in different plant model systems. *The Plant Cell*, *32*(11), 3388–3407. https://doi.org/10.1105/tpc.20.00235

Batsios, P., Meyer, I., & Graf, R. (2016). Proximity-dependent biotin identification (BioID) in *Dictyostelium amoebae*. *Methods in Enzymology*, *569*, 23–42. https://doi.org/10.1016/bs.mie.2015.09.007

Berggard, T., Linse, S., & James, P. (2007). Methods for the detection and analysis of protein–protein interactions. *Proteomics*, *7*(16), 2833–2842. https://doi.org/10.1002/pmic.200700131

Bhat, S. S., Bielewicz, D., Gulanicz, T., Bodi, Z., Yu, X., Anderson, S. J., Szewc, L., Bajczyk, M., Dolata, J., Grzelak, N., Smolinski, D. J., Gregory, B. D., Fray, R. G., Jarmolowski, A., & Szweykowska-Kulinska, Z. (2020). mRNA adenosine methylase (MTA) deposits m(6) a on pri-miRNAs to modulate miRNA biogenesis in *Arabidopsis thaliana*. *Proceedings of the National Academy of Sciences of the United States of America*, *117*(35), 21785–21795. https://doi.org/10.1073/pnas.2003733117

Boccaletto, P., Machnicka, M. A., Purta, E., Piatkowski, P., Baginski, B., Wirecki, T. K., de Crecy-Lagard, V., Ross, R., Limbach, P. A., Kotter, A., Helm, M., & Bujnicki, J. M. (2018). MODOMICS: A database of RNA modification pathways. 2017 update. *Nucleic Acids Research*, *46*(D1), D303–D307. https://doi.org/10.1093/nar/gkx1030

Branon, T. C., Bosch, J. A., Sanchez, A. D., Udeshi, N. D., Svinkina, T., Carr, S. A., Feldman, J. L., Perrimon, N., & Ting, A. Y. (2018). Efficient proximity labeling in living cells and organisms with TurboID. *Nature Biotechnology*, *36*(9), 880–887. https://doi.org/10.1038/nbt.4201

Bruckner, A., Polge, C., Lentze, N., Auerbach, D., & Schlattner, U. (2009). Yeast two-hybrid, a powerful tool for systems biology. *International Journal of Molecular Sciences*, *10*(6), 2763–2788. https://doi.org/10.3390/ijms10062763

Chen, A. L., Kim, E. W., Toh, J. Y., Vashisht, A. A., Rashoff, A. Q., Van, C., Huang, A. S., Moon, A. S., Bell, H. N., Bentolila, L. A., Wohlschlegel, J. A., & Bradley, P. J. (2015). Novel components of the toxoplasma inner membrane complex revealed by BioID. *MBio*, *6*, e02357–e02314. https://doi.org/10.1128/mBio.02357-14

Choi-Rhee, E., Schulman, H., & Cronan, J. E. (2004). Promiscuous protein biotinylation by *Escherichia coli* biotin protein ligase. *Protein Science*, *13*(11), 3043–3050. https://doi.org/10.1110/ps.04911804

Dunham, W. H., Mullin, M., & Gingras, A. C. (2012). Affinity-purification coupled to mass spectrometry: Basic principles and strategies. *Proteomics*, *12*(10), 1576–1590. https://doi.org/10.1002/pmic.201100523

Fashena, S. J., Serebriiskii, I., & Golemis, E. A. (2000). The continued evolution of two-hybrid screening approaches in yeast: How to outwit different preys with different baits. *Gene*, *250*, 1–14. https://doi.org/10.1016/S0378-1119(00)00182-7

Frye, M., Harada, B. T., Behm, M., & He, C. (2018). RNA modifications modulate gene expression during development. *Science*, *361*(6409), 1346–1349. https://doi.org/10.1126/science.aau1646

Fustin, J. M., Doi, M., Yamaguchi, Y., Hida, H., Nishimura, S., Yoshida, M., Isagawa, T., Morioka, M. S., Kakeya, H., Manabe, I., & Okamura, H. (2013). RNA-methylation-dependent RNA processing controls the speed of the circadian clock. *Cell*, *155*(4), 793–806. https://doi.org/10.1016/j.cell.2013.10.026

Gingras, A. C., Abe, K. T., & Raught, B. (2019). Getting to know the neighborhood: Using proximity-dependent biotinylation to characterize protein complexes and map organelles. *Current Opinion in Chemical Biology*, *48*, 44–54. https://doi.org/10.1016/j.cbpa.2018.10.017

Gingras, A. C., & Raught, B. (2012). Beyond hairballs: The use of quantitative mass spectrometry data to understand protein–protein interactions. *FEBS Letters*, *586*(17), 2723–2731. https://doi.org/10.1016/j.febslet.2012.03.065

Hamdi, A., & Colas, P. (2012). Yeast two-hybrid methods and their applications in drug discovery. *Trends in Pharmacological Sciences*, *33*(2), 109–118. https://doi.org/10.1016/j.tips.2011.10.008

Harrison, S. J., Mott, E. K., Parsley, K., Aspinall, S., Gray, J. C., & Cottage, A. (2006). A rapid and robust method of identifying transformed *Arabidopsis thaliana* seedlings following floral dip transformation. *Plant Methods*, *2*, 19. https://doi.org/10.1186/1746-4811-2-19

Hu, J., Cai, J., Park, S. J., Lee, K., Li, Y., Chen, Y., Yun, J. Y., Xu, T., & Kang, H. (2021). N(6) -Methyladenosine mRNA methylation is important for salt stress tolerance in *Arabidopsis*. *The Plant Journal*, *106*(6), 1759–1775. https://doi.org/10.1111/tpj.15270

Huang, H., Jedynak, B. M., & Bader, J. S. (2007). Where have all the interactions gone? Estimating the coverage of two-hybrid protein interaction maps. *PLoS Computational Biology*, *3*(11), e214. https://doi.org/10.1371/journal.pcbi.0030214

International Rice Genome Sequencing P. (2005). The map-based sequence of the rice genome. *Nature*, *436*(7052), 793–800. https://doi.org/10.1038/nature03895

Ke, S., Alemu, E. A., Mertens, C., Gantman, E. C., Fak, J. J., Mele, A., Haripal, B., Zucker-Scharff, I., Moore, M. J., Park, C. Y., Vagbo, C. B., Kussnierczyk, A., Klungland, A., Darnell, J. E. Jr., & Darnell, R. B. (2015). A majority of m6A residues are in the last exons, allowing the potential for 3' UTR regulation. *Genes & Development*, *29*(19), 2037–2053. https://doi.org/10.1101/gad.269415.115

Keskin, O., Tuncbag, N., & Gursoy, A. (2016). Predicting protein–protein interactions from the molecular to the proteome level. *Chemical Reviews*, *116*(8), 4884–4909. https://doi.org/10.1021/acs.chemrev.5b00683

Khan, M., Youn, J. Y., Gingras, A. C., Subramaniam, R., & Desveaux, D. (2018). In planta proximity dependent biotin identification (BioID). *Scientific Reports*, *8*(1), 9212. https://doi.org/10.1038/s41598-018-27500-3

Kim, D. I., Jensen, S. C., Noble, K. A., Kc, B., Roux, K. H., Motamedchaboki, K., & Roux, K. J. (2016). An improved smaller biotin ligase for BioID proximity labeling. *Molecular Biology of the Cell*, *27*(8), 1188–1196. https://doi.org/10.1091/mbc.E15-12-0844

Knuckles, P., Lence, T., Haussmann, I. U., Jacob, D., Kreim, N., Carl, S. H., Masiello, I., Hares, T., Villasenor, R., Hess, D., Andrade-Navarro, M. A., Biggiogera, M., Helm, M., Soller, M., Buhler, M., & Roignant, J. Y. (2018). Zc3h13/Flacc is required for adenosine methylation by bridging the mRNA-binding factor Rbm15/Spenito to the m(6)a machinery component Wtap/Fl(2)d. *Genes & Development*, *32*(5–6), 415–429. https://doi.org/10.1101/gad.309146.117

Liu, F., Rijkers, D. T., Post, H., & Heck, A. J. (2015). Proteome-wide profiling of protein assemblies by cross-linking mass spectrometry. *Nature Methods*, *12*(12), 1179–1184. https://doi.org/10.1038/nmeth.3603

Mair, A., & Bergmann, D. C. (2022). Advances in enzyme-mediated proximity labeling and its potential for plant research. *Plant Physiology*, *188*(2), 756–768. https://doi.org/10.1093/plphys/kiab479

Mair, A., Xu, S. L., Branon, T. C., Ting, A. Y., & Bergmann, D. C. (2019). Proximity labeling of protein complexes and cell-type-specific organellar proteomes in *Arabidopsis* enabled by TurboID. *eLife*, *8*, e47864. https://doi.org/10.7554/eLife.47864

Martell, J. D., Deerinck, T. J., Sancak, Y., Poulos, T. L., Mootha, V. K., Sosinsky, G. E., Ellisman, M. H., & Ting, A. Y. (2012). Engineered ascorbate peroxidase as a genetically encoded reporter for electron microscopy. *Nature Biotechnology*, *30*(11), 1143–1148. https://doi.org/10.1038/nbt.2375

Opitz, N., Schmitt, K., Hofer-Pretz, V., Neumann, B., Krebber, H., Braus, G. H., & Valerius, O. (2017). Capturing the Asc1p/receptor for activated C kinase 1 (RACK1) microenvironment at the head region of the 40S ribosome with quantitative BioID in yeast. *Molecular & Cellular Proteomics*, *16*(12), 2199–2218. https://doi.org/10.1074/mcp.M116.066654

Ramanathan, M., Majzoub, K., Rao, D. S., Neela, P. H., Zarnegar, B. J., Mondal, S., Roth, J. G., Gai, H., Kovalski, J. R., Siprashvili, Z., Palmer, T. D., Carette, J. E., & Khavari, P. A. (2018). RNA-protein interaction detection in living cells. *Nature Methods*, *15*(3), 207–212. https://doi.org/10.1038/nmeth.4601

Roux, K. J., Kim, D. I., Raida, M., & Burke, B. (2012). A promiscuous biotin ligase fusion protein identifies proximal and interacting proteins in mammalian cells. *The Journal of Cell Biology*, *196*(6), 801–810. https://doi.org/10.1083/jcb.201112098

Schmidtmann, E., Anton, T., Rombaut, P., Herzog, F., & Leonhardt, H. (2016). Determination of local chromatin composition by CasID. *Nucleus*, *7*(5), 476–484. https://doi.org/10.1080/19491034.2016.1239000

Shen, L., Liang, Z., Gu, X., Chen, Y., Teo, Z. W., Hou, X., Cai, W. M., Dedon, P. C., Liu, L., & Yu, H. (2016). N(6)-Methyladenosine RNA modification regulates shoot stem cell fate in *Arabidopsis*. *Developmental Cell*, *38*(2), 186–200. https://doi.org/10.1016/j.devcel.2016.06.008

Vespa, L., Vachon, G., Berger, F., Perazza, D., Faure, J. D., & Herzog, M. (2004). The immunophilin-interacting protein AtFIP37 from *Arabidopsis* is essential for plant development and is involved in trichome endoreduplication. *Plant Physiology*, *134*(4), 1283–1292. https://doi.org/10.1104/pp.103.028050

Wang, X., Jiang, B., Gu, L., Chen, Y., Mora, M., Zhu, M., Noory, E., Wang, Q., & Lin, C. (2021). A photoregulatory mechanism of the circadian clock in *Arabidopsis*. *Nat Plants*, *7*(10), 1397–1408. https://doi.org/10.1038/s41477-021-01002-z

Wen, J., Lv, R., Ma, H., Shen, H., He, C., Wang, J., Jiao, F., Liu, H., Yang, P., Tan, L., Lan, F., Shi, Y. G., He, C., Shi, Y., & Diao, J. (2018). Zc3h13 regulates nuclear RNA m(6)a methylation and mouse embryonic stem cell self-renewal. *Molecular Cell*, *69*(6), 1028–1038 e1026. https://doi.org/10.1016/j.molcel.2018.02.015

Yang, X., Wen, Z., Zhang, D., Li, Z., Li, D., Nagalakshmi, U., Dinesh-Kumar, S. P., & Zhang, Y. (2021). Proximity labeling: An emerging tool for probing in planta molecular interactions. *Plant Community*, *2*(2), 100137. https://doi.org/10.1016/j.xplc.2020.100137

Yue, H., Nie, X., Yan, Z., & Weining, S. (2019). N6-methyladenosine regulatory machinery in plants: Composition, function and evolution. *Plant Biotechnology Journal*, *17*(7), 1194–1208. https://doi.org/10.1111/pbi.13149

Zhang, M., Bodi, Z., Mackinnon, K., Zhong, S., Archer, N., Mongan, N. P., Simpson, G. G., & Fray, R. G. (2022). Two zinc finger proteins with functions in m(6)A writing interact with HAKAI. *Nature Communications*, *13*(1), 1127. https://doi.org/10.1038/s41467-022-28753-3

Zhang, Y., Song, G., Lal, N. K., Nagalakshmi, U., Li, Y., Zheng, W., Huang, P. J., Branon, T. C., Ting, A. Y., Walley, J. W., & Dinesh-Kumar, S. P. (2019). TurboID-based proximity labeling reveals that UBR7 is a regulator of N NLR immune receptor-mediated immunity. *Nature Communications*, *10*(1), 3252. https://doi.org/10.1038/s41467-019-11202-z

Zhao, B. S., Roundtree, I. A., & He, C. (2017). Post-transcriptional gene regulation by mRNA modifications. *Nature Reviews. Molecular Cell Biology*, *18*(1), 31–42. https://doi.org/10.1038/nrm.2016.132

Zhong, S., Li, H., Bodi, Z., Button, J., Vespa, L., Herzog, M., & Fray, R. G. (2008). MTA is an *Arabidopsis* messenger RNA adenosine methylase and interacts with a homolog of a sex-specific splicing factor. *Plant Cell*, *20*(5), 1278–1288. https://doi.org/10.1105/tpc.108.058883

SUPPORTING INFORMATION

Additional supporting information can be found online in the Supporting Information section at the end of this article.

How to cite this article: Li, X., Wei, Y., Fei, Q., Fu, G., Gan, Y., & Shi, C. (2023). TurboID-mediated proximity labeling for screening interacting proteins of FIP37 in *Arabidopsis*. *Plant Direct*, *7*(12), e555. https://doi.org/10.1002/pld3.555